

Core-shell diamond-like silicon photonic crystals from 3D polymer templates created by holographic lithography

Jun Hyuk Moon and Shu Yang

Department of Materials Science and Engineering, University of Pennsylvania,
3231 Walnut Street, Philadelphia, PA 19104
shuyang@seas.upenn.edu

Wenting Dong and Joseph W. Perry

School of Chemistry and Biochemistry, Georgia Institute of Technology, Atlanta, GA 30332

Ali Adibi

School of Electrical and Computer Engineering, Georgia Institute of Technology, Atlanta, GA 30332

Seung-Man Yang

National Creative Research Initiative Center for Integrated Optofluidic Systems and Department of Chemical and Biomolecular Engineering, Korea Advanced Institute of Science and Technology, 305-701 Guseong-dong, Yuseong-gu, Daejeon, Korea

Abstract: We have fabricated diamond-like silicon photonic crystals through a sequential silica/silicon chemical vapor deposition (CVD) process from the corresponding polymer templates photopatterned by holographic lithography. Core-shell morphology is revealed due to the partial backfilling of the interstitial pores. To model the shell formation and investigate its effect to the bandgap properties, we developed a two-parameter level-set approach that closely approximated the core-shell morphology, and compare the bandgap simulation with the measured optical properties of the 3D crystals at each processing step. Both experimental and calculation results suggest that a complete filling is necessary to maximize the photonic bandgap in the diamond-like structures.

©2006 Optical Society of America

OCIS codes: (999.9999) Photonic crystal, (090.0090) Holography; (260.3160) Interference; (220.4000) Microstructure fabrication

References and links

1. V. N. Astratov, V. N. Bogomolov, A. A. Kaplyanskii, A. V. Prokofiev, L. A. Samoilovich, S. M. Samoilovich, and Y. A. Vlasov, "Optical spectroscopy of opal matrices with CdS embedded in its pores: Quantum confinement and photonic band gap effects," *Nuovo Cimento Soc. Ital. Fis. D-Condens. Matter At. Mol. Chem. Phys. Fluids Plasmas Biophys.* **17**, 1349-1354 (1995).
2. S. Y. Lin, J. G. Fleming, D. L. Hetherington, B. K. Smith, R. Biswas, K. M. Ho, M. M. Sigalas, W. Zubrzycki, S. R. Kurtz, and J. Bur, "A three-dimensional photonic crystal operating at infrared wavelengths," *Nature* **394**, 251-253 (1998).
3. M. Campbell, D. N. Sharp, M. T. Harrison, R. G. Denning, and A. J. Turberfield, "Fabrication of photonic crystals for the visible spectrum by holographic lithography," *Nature* **404**, 53-56 (2000).
4. G. M. Gratson, M. J. Xu, and J. A. Lewis, "Microporoidis structures - Direct writing of three-dimensional webs," *Nature* **428**, 386-386 (2004).
5. A. Blanco, E. Chomski, S. Grachtak, M. Ibsate, S. John, S. W. Leonard, C. Lopez, F. Meseguer, H. Miguez, J. P. Mondia, G. A. Ozin, O. Toader, and H. M. van Driel, "Large-scale synthesis of a silicon photonic crystal with a complete three-dimensional bandgap near 1.5 micrometres," *Nature* **405**, 437-440 (2000).
6. S. Shoji, and S. Kawata, "Photofabrication of three-dimensional photonic crystals by multibeam laser interference into a photopolymerizable resin," *Appl. Phys. Lett.* **76**, 2668-2670 (2000).

7. S. Noda, K. Tomoda, N. Yamamoto, and A. Chutinan, "Full three-dimensional photonic bandgap crystals at near-infrared wavelengths," *Science* **289**, 604-606 (2000).
8. J. H. Moon, J. Ford, and S. Yang, "Fabricating three-dimensional polymer photonic structures by multi-beam interference lithography," *Polym. Adv. Technol.* **17**, 83-93 (2006).
9. Y. V. Miklyaev, D. C. Meisel, A. Blanco, G. von Freymann, K. Busch, W. Koch, C. Enkrich, M. Deubel, and M. Wegener, "Three-dimensional face-centered-cubic photonic crystal templates by laser holography: fabrication, optical characterization, and band-structure calculations," *Appl. Phys. Lett.* **82**, 1284-1286 (2003).
10. S. Yang, M. Megens, J. Aizenberg, P. Wiltzius, P. M. Chaikin, and W. B. Russel, "Creating periodic three-dimensional structures by multibeam interference of visible laser," *Chem. Mater.* **14**, 2831-2833 (2002).
11. R. L. Sutherland, V. P. Tondiglia, L. V. Natarajan, S. Chandra, D. Tomlin, and T. J. Bunning, "Switchable orthorhombic *F* photonic crystals formed by holographic polymerization-induced phase separation of liquid crystal," *Opt. Express* **10**, 1074-1082 (2002).
12. C. K. Ullal, M. Maldovan, E. L. Thomas, G. Chen, Y. J. Han, and S. Yang, "Photonic crystals through holographic lithography: Simple cubic, diamond-like, and gyroid-like structures," *Appl. Phys. Lett.* **84**, 5434-5436 (2004).
13. S. P. Gorkhali, J. Qi, and G. P. Crawford, "Electrically switchable mesoscale Penrose quasicrystal structure," *Appl. Phys. Lett.* **86**, 011110 (2005).
14. X. Wang, C. Y. Ng, W. Y. Tam, C. T. Chan, and P. Sheng, "Large-area two-dimensional mesoscale quasicrystals," *Adv. Mater.* **15**, 1526-1528 (2003).
15. M. Maldovan, A. M. Urbas, N. Yufa, W. C. Carter, and E. L. Thomas, "Photonic properties of bicontinuous cubic microphases," *Phys. Rev. B* **65**, 165123 (2002).
16. C. K. Ullal, M. Maldovan, M. Wohlgenuth, and E. L. Thomas, "Triply periodic bicontinuous structures through interference lithography: a level-set approach," *J. Opt. Soc. Am. A* **20**, 948-954 (2003).
17. Y. A. Vlasov, X. Z. Bo, J. C. Sturm, and D. J. Norris, "On-chip natural assembly of silicon photonic bandgap crystals," *Nature* **414**, 289-293 (2001).
18. H. Miguez, N. Tetreault, S. M. Yang, V. Kitaev, and G. A. Ozin, "A new synthetic approach to silicon colloidal photonic crystals with a novel topology and an omni-directional photonic bandgap: Micromolding in inverse silica opal (MISO)," *Adv. Mater.* **15**, 597-600 (2003).
19. N. Tetreault, H. Miguez, and G. A. Ozin, "Silicon inverse opal - A platform for photonic bandgap research," *Adv. Mater.* **16**, 1471-1476 (2004).
20. A. Blanco, and C. López, "Silicon onion-layer nanostructures arranged in three dimensions," *Adv. Mater.*, In press (2006).
21. H. Miguez, N. Tetreault, B. Hatton, S. M. Yang, D. Perovic, and G. A. Ozin, "Mechanical stability enhancement by pore size and connectivity control in colloidal crystals by layer-by-layer growth of oxide," *Chem. Commun.*, 2736-2737 (2002).
22. G. M. Gratson, F. Garcia-Santamaria, V. Lousse, M. J. Xu, S. H. Fan, J. A. Lewis, and P. V. Braun, "Direct-write assembly of three-dimensional photonic crystals: Conversion of polymer scaffolds to silicon hollow-woodpile structures," *Adv. Mater.* **18**, 461-465 (2006).
23. N. Tetreault, G. von Freymann, M. Deubel, M. Hermatschweiler, F. Pérez-Willard, S. John, M. Wegener, and G. A. Ozin, "New route to three-dimensional photonic bandgap materials: Silicon double inversion of polymer templates," *Adv. Mater.* **18**, 457-460 (2006).
24. K. Busch, and S. John, "Photonic band gap formation in certain self-organizing systems," *Phys. Rev. E* **58**, 3896-3908 (1998).
25. J. H. Moon, S.-M. Yang, and S. Yang, "Photonic bandgap structures of core-shell simple cubic crystals from Holographic Lithography," *Appl. Phys. Lett.* **88**, 121101 (2006).
26. H. M. Su, Y. C. Zhong, X. Wang, X. G. Zheng, J. F. Xu, and H. Z. Wang, "Effects of polarization on laser holography for microstructure fabrication," *Phys. Rev. E* **67** (2003).
27. The calculated bandgap width is smaller than literature value, which may be attributed to the discrepancy in refractive index of silicon used in calculation and calculation resolution.

1. Introduction

The concept of three-dimensional (3D) photonic crystals (PCs) [1] that possess an omnidirectional bandgap in the optical regime has stimulated extensive research on discovery of novel fabrication methods [2-6], and on the study of the photonic bandgap (PBG) properties of such produced structures as novel photonic and optoelectronic materials [7]. Among many 3D microfabrication methods, holographic lithography (HL) is fast and flexible to achieve a wide range of lattices [8], including face-centered cubic [9], diamond-like [3, 10], orthorhombic *F* [11], simple cubic and gyroid-like structure [12], as well as quasicrystals [13, 14]. The lattice and basis can be precisely controlled by the beam geometry, polarization, phase, intensity, and wavelength and the resulting 3D crystals often possess large and robust

photonic bandgap (PBG) [15, 16]. However, most holographic 3D structures are produced in polymers or low-index inorganic materials, which do not show complete photonic bandgap.

Of many high index materials silicon is ideal because of its high refractive index ($n= 3.5 - 3.9$) and transparency in the near-IR and IR region. Recently several groups have investigated the fabrication of silicon photonic crystals through silicon chemical vapor deposition (CVD) of synthetic opals from silica [17-19], and polymers [20], or a double templating method using a sequential silica [21] /silicon [17-19] CVD process from polymeric wood-piles structures fabricated by direct-write assembly [22] and direct-laser writing [23], respectively. Core-shell morphology is often revealed during the CVD process when the deposited materials grow continuously on the 3D template surface to fill the interstitial pores. It has been suggested that an optimized shell thickness in the face-centered cubic [24] and simple cubic structures [25] can enhance the complete bandgap between 5th and 6th bands and 8th and 9th bands, respectively; while a lower reflectance has been observed in the hollow-woodpile Si structures due to partial filling [22].

Thus, a quantitative understanding of the nanostructure of the 3D crystals, in particular those fabricated by holographic lithography, at each processing step is crucial if one wishes to exploit their unique optical properties in novel photonic materials. To this end, we have carried out the double-templating method to fabricate diamond-like silicon photonic crystals from the polymer templates. To model the shell formation and investigate its effect to the bandgap properties, we have developed a two-parameter level-set approach that closely approximates the core-shell structures, and compare the bandgap simulation with the measured optical properties of the 3D crystals at each processing step. Both results suggest that a complete filling is necessary to maximize PBGs in the diamond-like structures.

2. Fabrication of polymer, silica, and silicon photonic crystals by holographic lithography

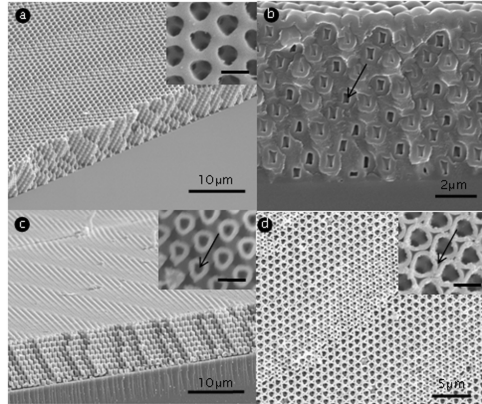


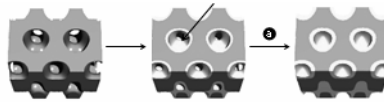
Fig. 1. SEM images of (a) diamond-like SU-8 structures, inverse silica replica before (b) and after (c) the removal of the template, and (d) silicon diamond-like photonic crystals. Insets in (a), (c), and (d) show the (111) plane. Scale bar: 1 μ m. The arrows in (b) and (c) indicate the unfilled air voids.

In the HL experiment to fabricate the polymer templates, we constructed four umbrella-like beams to create an interference pattern with three-term diamond-like symmetry [12, 26]. A laser beam source ($\lambda=532\text{nm}$, Power Diode-Pumped Nd:YVO4 Laser, Coherent) was split into four beams to produce an interference pattern. The central beam was circularly polarized and incident perpendicularly to the photoresist film. The other three beams were oblique at 39° relative to the central beam and polarized linearly in a plane formed by the wavevectors of the central beam and surrounding beam. The wave vectors of each beam are $k_0=\pi/a[333]$, $k_1=\pi/a[511]$, $k_2=\pi/a[151]$, and $k_3=\pi/a[115]$. The polarization vectors of beam 1, 2, and 3

are $e_1=[0.680\ 0.680\ -0.272]$, $e_2=[0.680\ -0.272\ 0.680]$, and $e_3=[-0.272\ 0.680\ 0.680]$. The intensity ratio between the central beam and the surrounding beams was 3.6:1:1:1. It was predicted that such diamond-like structure possessed a complete and robust bandgap between the 2nd and 3rd bands, and the 7th and 8th bands [12].

The superposed interference intensity profile can be approximated by $I(x,y,z) \propto \sin(x+y-z) + \sin(x-y+z) + \sin(-x+y+z)$ [12]. The interference pattern was then transferred to a SU-8 photoresist film with an average exposure dose of 0.2 – 0.5 J/cm². After post-exposure bake, the sample was developed in propylene glycol monomethyl ether acetate (PGMEA), followed by supercritical CO₂ drying to prevent pattern collapse [10]. Since the laser beam has a Gaussian distribution of intensity, the volume fraction of polymer decreases towards the edge of the interference pattern. Figure 1(a) shows a representative scanning electron microscopy (SEM) image of a diamond-like polymer structure in the center region of the patterned film.

Since silicon deposition requires a high processing temperature (> 400°C), which will decompose the polymer template, the polymer PC was first converted to a silica inverse structure through consecutive exposures to SiCl₄ vapor and water vapor using atmospheric pressure at room temperature [21]. The silica layer was formed continuously and extended layer-by-layer to fill the interstitial pores. By fine-control of the reaction rate, the silica structures show high mechanical stability without disrupting the connectivity and long range order of the polymer templates [21-23]. In our experiment, the deposition was repeated 4-5 times to nearly fill the pores. As shown in Fig. 1(b) of the silica-polymer composite, unfilled, isolated air voids were observed as indicated by the arrow. They were formed due to the inability to further access the internal voids by SiCl₄ vapor once the pores connecting these voids were closed during the CVD reaction (see Scheme 1). After calcination of polymer template at 500°C, an inverted silica structure with 200-250 nm thick shell was obtained [see Fig. 1(c)].



Scheme 1. Deposition of silica on the polymer template. (a) The pores into the internal voids are closed during the deposition before filling the voids completely.

The top surface that was completely covered with silica after the CVD was removed by reactive-ion etching for the subsequent silicon backfilling. Through low pressure chemical vapor deposition (LPCVD) of silane (SiH₄) gas at 550 °C, a 150 – 200 nm thick silicon layer was deposited at a rate of 100-150 nm/hour. The silicon-silica composite was mounted on a sapphire substrate using an optical adhesive [23] and the silica was etched away using 1-5% HF solution. Figure 1(d) shows the SEM images of silicon photonic crystal and the magnified (111) plane, respectively.

3. Optical characterization of core-shell diamond-like photonic crystals

The reflectance in the (111) direction of the polymer, silica, and silicon PCs at each processing step were measured using an FT-IR equipped with an infrared microscope. The SU-8 structure had a reflection peak at 2.4 – 2.6 μm, corresponding to a volume fraction of 0.40 – 0.60, which was estimated by Bragg's law using the lattice distance in (111) direction ($d_{111} = 0.92 - 0.94 \mu\text{m}$ by SEM image analysis) and the refractive index of SU-8, $n = 1.6$. The reflection peak frequency varied 10 % over the patterned area, which could be attributed to the Gaussian distribution of the beam intensity along the beam diameter.

Since a shell layer is formed during the silica and silicon CVD process, respectively, it is essential to develop a quantitative model that studies the effect of core-shell morphology to the photonic bandgap properties. The comparison between the measured optical properties to the calculated photonic band structures at each processing step will offer important guidance for the fabrication of 3D photonic crystals, in particular, the diamond and diamond-like

crystals, which have shown large and complete photonic bandgap. For bandgap calculation, we constructed a level surface of the physical structure from the superimposed intensity of interference terms, $I(x,y,z)$. Since the optical measurement suggests that all the crystals we fabricated (polymer, silica and core-shell silicon crystals) show incomplete photonic bandgap, here we only discuss the calculation of L-gap to better illustrate the model we developed. Based on the SEM images [Fig. 1(a)], the polymer 3D structure has a volume fraction of 0.47 and can be approximated using $0.1 < I(x,y,z)$. Thus constructed level surface of the structure is shown in the inset of Fig. 2(a). As seen in Fig. 2(a), the position of normalized reflection peak, $a/\lambda=0.65$, for the polymer structure aligns well with the calculated pseudogap between the 2nd and 3rd bands, which corresponds to the ΓL direction (L-gap).

After calcination, the d_{111} of the silica structure decreased by 10 – 15 % to 0.80 – 0.83 μm . The reflection peaks from the L-gap was shifted to 1.8 μm as expected due to the smaller lattice period and lower refractive index of silica, $n = 1.4$, compared to that of SU-8. The volume fraction was estimated to be in the range of 0.30 – 0.35. Since a conformal silica shell was grown continuously along the normal to the initial surface, we introduce a two-parameter level-set approach that approximates the core-shell structure as

$$t_1 < I(x,y,z) < t_2 \text{ for the dielectric regions surrounded by air, and} \\ t_1 > I(x,y,z) \text{ and } t_2 < I(x,y,z) \text{ for air,}$$

where t_1 and t_2 are two parallel level surfaces that represent the newly grown surface and the template surface, respectively, or vice versa [25]. Here t_2 represents the polymer structure, approximated as 0.1. Based on the calculated volume fraction and the SEM image analysis, t_1 is estimated as -1.0. Accordingly, the silica structure is defined by $-1.0 < I(x,y,z) < 0.1$ [see inset in Fig. 2(b)]. The calculated pseudogap in the silica photonic crystal matches well with the measured peak in the reflectance spectrum [Fig. 2(b)].

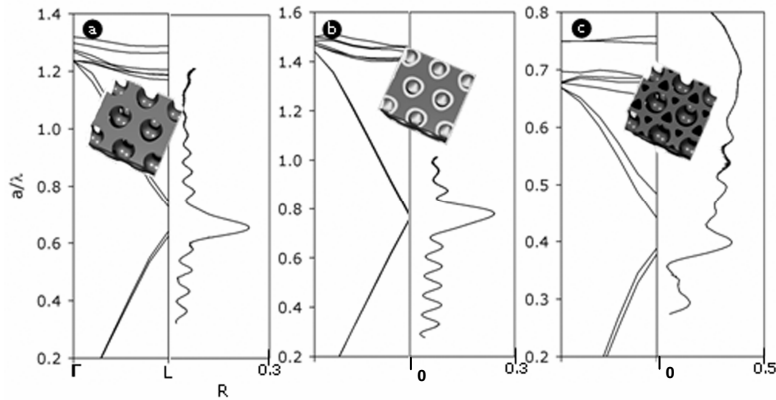


Fig. 2. Photonic band structure and normalized reflectance spectra for (a) SU-8, (b) silica, and (c) silicon photonic crystals. Insets show the level surface of (a) polymer, and level surfaces of (b) polymer (grey) and silica (white) and (c) silicon (grey) and air voids (black): (a) $0.1 < I$, (b) $-1.0 < I < 0.1$, and (c) $0.1 < I < 1.4$.

For the silicon structure, the reflectance peaked at 3.6 μm in the (111) direction, but did not show complete photonic bandgap along all relevant directions. The volume fraction was estimated as 0.32 – 0.36 given the refractive index of silicon, $n = 3.55$, and the lattice spacing, $d_{111} = 0.80 - 0.83$. In this case, t_1 is the level surface of the silica template and t_2 is estimated as 1.4 using the above calculation approximation. Thus, the silicon structure can be described as $0.1 < I(x,y,z) < 1.4$ [see inset in Fig. 1(c)], which possess a volume fraction of 0.34. As shown in Fig. 2(c), the calculated band structures in ΓL direction agree well with the measured reflection peak from the L-gap. However, the bandgap between 2nd and 3rd bands were found closed in the core-shell silicon photonic crystals.

Since the light intensity of the laser beam has Gaussian distribution across the film diameter, the fabricated silicon crystal deviates from an ideal level surface, $0.4 < I(x,y,z)$. To verify the effect of core-shell morphology to the bandgap properties we recalculate the bandgap structure using an optimized silicon diamond-like structure ($t_1 = 0.4$ and $0.4 < I(x,y,z)$) with variable shell thickness (namely t_2).

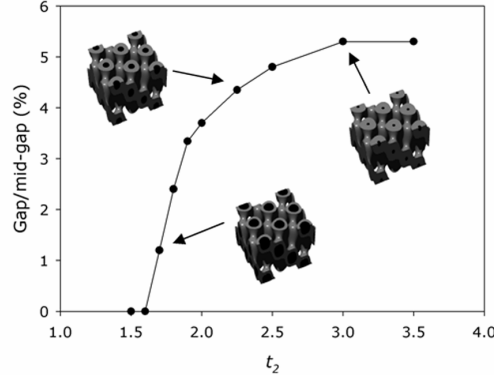


Fig. 3. Gap/mid-gap width of core-shell diamond-like photonic crystals as a function of a threshold value t_2 . Two level surfaces are defined by two threshold values of $t_1 = 0.4$ and t_2 , and the shell structure are defined by $0.4 < I < t_2$. Inset: 3D structures defined by $t_1=0.4$ (grey) and the corresponding t_2 (black).

As seen in Fig. 3, the bandgap has a maximum when the structure is completely filled and decreases as the shell thickness decreases (i.e., t_2 decreases) [27]. Therefore, it explains the observation of incomplete bandgap in the fabricated core-shell silicon photonic crystals. This behavior differs from the reported findings in the case of simple cubic and face-centered cubic structures, where the core-shell morphologies are shown to enhance complete bandgap between 5th and 6th bands, and 8th and 9th bands, respectively [24, 25].

4. Conclusion

We have demonstrated the fabrication of diamond-like silicon photonic crystals templated from the holographically-patterned polymer structures. During the sequential silica/silicon chemical vapor deposition process, a core-shell structure was revealed due to the incomplete backfilling. To quantitatively study the effect of shell thickness to the photonic bandgap properties, we developed a two-parameter level-set approach to model the core-shell morphology and compared the calculated bandgap structures with the measured reflectance of the 3D crystals (polymer, silica and silicon) at each processing step. Both experimental and calculation results suggest that a complete filling is necessary to maximize the photonic bandgap in the diamond-like structures fabricated by holographic lithography. This study provides the first quantitative analysis of the formation of core-shell Si photonic crystals through templating, and suggests the importance of control over the crystal fabrication and CVD processing parameters to the bandgap properties. Such understanding is crucial to apply the templating approach for the fabrication of a wide range of high index photonic crystals.

Acknowledgments

This work is supported by the Office of Naval Research (ONR), Grant # N00014-05-0303, and the Korea Research Foundation postdoc fellowship (JHM), Grant # KRF-2005-000-10299. SMY acknowledges supports from the Creative Research Initiative Program of MOST/KOSEF and the BK21 Program of MOE & HRD. The authors would like to thank Gary Spinner for silicon deposition at the MiRC at Georgia Institute of Technology, and Vincent Chen and Babak Momeni at Georgia Institute of Technology for useful discussions.